

## Designed Peptides with Homochiral and Heterochiral Diproline Templates as Conformational Constraints

Bhaswati Chatterjee,<sup>[a]</sup> Indranil Saha,<sup>[b]</sup> Srinivasarao Raghothama,<sup>[c]</sup>  
 Subrayashastry Aravinda,<sup>[b]</sup> Rajkishor Rai,<sup>[a]</sup> Narayanaswamy Shamala,<sup>\*[b]</sup> and  
 Padmanabhan Balaram<sup>\*[a]</sup>

**Abstract:** Diproline segments have been advanced as templates for nucleation of folded structure in designed peptides. The conformational space available to homochiral and heterochiral diproline segments has been probed by crystallographic and NMR studies on model peptides containing L-Pro-L-Pro and D-Pro-L-Pro units. Four distinct classes of model peptides have been investigated: a) isolated D-Pro-L-Pro segments which form type II'  $\beta$ -turn; b) D-Pro-L-Pro-L-Xxx sequences which form type II'-I ( $\beta_{II'-I}$ , consecutive  $\beta$ -turns) turns; c) D-Pro-L-Pro-D-Xxx sequences; d) L-Pro-L-Pro-L-Xxx sequences. A total of 17 peptide crystal

structures containing diproline segments are reported. Peptides of the type Piv-D-Pro-L-Pro-L-Xxx-NHMe are conformationally homogeneous, adopting consecutive  $\beta$ -turn conformations. Peptides in the series Piv-D-Pro-L-Pro-D-Xxx-NHMe and Piv-L-Pro-L-Pro-L-Xxx-NHMe, display a heterogeneity of structures in crystals. A type VIa  $\beta$ -turn conformation is characterized in Piv-L-Pro-L-Pro-L-Phe-OMe (**18**), while an example of a 5 $\rightarrow$ 1 hydrogen


bonded  $\alpha$ -turn is observed in crystals of Piv-D-Pro-L-Pro-D-Ala-NHMe (**11**). An analysis of pyrrolidine conformations suggests a preferred proline puckering geometry is favored only in the case of heterochiral diproline segments. Solution NMR studies, reveal a strong conformational influence of the C-terminal Xxx residues on the structures of diproline segments. In L-Pro-L-Pro-L-Xxx sequences, the Xxx residues strongly determine the population of Pro-Pro *cis* conformers, with an overwhelming population of the *trans* form in L-Xxx = L-Ala (**19**).

**Keywords:** beta turns • conformation analysis • peptide folding • peptides

[a] B. Chatterjee, R. Rai, Prof. P. Balaram  
 Molecular Biophysics Unit, Indian Institute of Science  
 Bangalore 560012 (India)  
 Fax: (+91)80-2360-0683  
 E-mail: pb@mbu.iisc.ernet.in

[b] I. Saha, S. Aravinda, Prof. N. Shamala  
 Department of Physics, Indian Institute of Science  
 Bangalore 560012 (India)  
 Fax: (+91)80-23602602  
 E-mail: shamala@physics.iisc.ernet.in

[c] S. Raghothama  
 NMR Research Centre, Indian Institute of Science  
 Bangalore 560012 (India)

 Supporting information for this article is available on the WWW under <http://www.chemeurj.org/> or from the author: Crystal and diffraction data and refinement details (Table S2); intramolecular hydrogen-bond parameters (Table S3), the puckering analysis of proline rings (Tables S4–S6) and the packing diagrams for peptides **1–8**, **10–15**, **18**, **20** and **23** (Figures S7–S11); general procedures for peptide synthesis of representative compounds **1**, **9**, **11**; *m/z* values in ESI-MS spectra (positive ion mode) for the peptides **1–23** (Table S1), ESI-MS spectra (positive ion mode) for all **1–23** peptides (Figures S1–S6), <sup>13</sup>C chemical shifts for the peptides Piv-L-Pro-L-Pro-L-Xxx-NHMe in CDCl<sub>3</sub> (Table S7).

### Introduction

Diproline segments have emerged as important templates in the design of synthetic peptides with defined structures. While homochiral L-Pro-L-Pro segments have been advanced as potential nucleator of helical conformations,<sup>[1]</sup> the heterochiral D-Pro-L-Pro segments are effective templates for  $\beta$ -hairpin formation.<sup>[2]</sup> Proline is unique among the 20 genetically coded amino acids in possessing a covalent linkage between the side chain and the backbone nitrogen atom. The direct consequence of the formation of the pyrrolidine ring, is the restriction imposed on the torsional freedom about the N–C $\alpha$  bond, limiting the dihedral angle  $\phi$  to values of  $-60 \pm 30^\circ$  for L-Pro. The restraint imposed on conformational freedom makes proline the most frequently observed residue in turn segments of proteins<sup>[3]</sup> and also the most widely used residue in the design of well structured peptides.<sup>[4]</sup> Three distinct conformations have been characterized, corresponding to i) polyproline (P<sub>II</sub>,  $\phi \sim -70^\circ$ ,  $\psi \sim +120^\circ$ ), ii)  $\gamma$ -turn (C<sub>7</sub>,  $\phi \sim -70^\circ$ ,  $\psi \sim +70^\circ$ ) and iii) helical ( $\alpha_R$ ,

$\phi \sim -60^\circ$ ,  $\psi \sim -30^\circ$ ) structures. Proline has been considered as a secondary structure breaker in proteins and is generally disfavored in both regular  $\alpha$ -helices and  $\beta$ -sheets.<sup>[5]</sup> This is largely a consequence of the absence of the NH group, impeding intramolecular hydrogen bonding, an interaction characteristic of polypeptide secondary structures. Proline is however observed at the N-terminus (N-cap) region of helices.<sup>[6]</sup> This is readily rationalized by the fact that the backbone torsion angles required for  $\alpha$ -helix formation are readily adopted by proline and that the N-terminus NH group does not participate in intramolecular hydrogen bonding. Proline is indeed a more decisive breaker of  $\beta$ -sheets, where both the hydrogen bonding and torsion angle requirements are not accommodated. The use of proline containing peptides, which inhibit amyloid fibre formation is a notable example in which the poor  $\beta$ -sheet forming propensity of this residue has been cleverly exploited.<sup>[7]</sup> In proteins, proline occurs widely in loops and in the turn regions which facilitate polypeptide chain reversal, thus permitting the formation of globular structures. Two residue turns ( $\beta$ -turns) are the best characterized short range structural features in proteins. Since their original description by Venkatachalam, nearly four decades ago, based on an analysis of the sterically allowed intramolecular hydrogen bonded conformation of the three linked *trans* planar peptide units,<sup>[8]</sup> a wide variety of  $\beta$ -turn families have been characterized in protein crystal structures.<sup>[3b]</sup> Several insights have emerged from this large body of published work. Notably, L-Pro has the greatest propensity among the twenty genetically coded amino acids to occur at the  $i+1$  position of type I/III and type II  $\beta$ -turns. When proline occurs at the  $i+2$  position, the preceding X-Pro peptide bond is invariably *cis* and the resultant intramolecular 4 $\rightarrow$ 1 hydrogen bonded structure has been termed as a type VI  $\beta$ -turn.<sup>[3b]</sup> These conformational properties of proline residues have stimulated a large number of studies directed towards the use of proline containing sequences in the “first principles design” of folded peptide structures.

Diproline segments constitute a chain fragment with considerably reduced conformational choices. Figure 1, illustrates the allowed regions of  $\phi$ ,  $\psi$  space for both L- and D-proline residues. The possible conformations of both homochiral and heterochiral diproline segments are indicated, allowing a choice of only P<sub>II</sub>/P<sub>II</sub>' and  $\alpha_L/\alpha_R$  conformations. In a study published as early as 1979 from this laboratory, a two hydrogen bonded conformation was proposed for the model sequence Piv-L-Pro-L-Pro-L-Ala-NHMe. The conformation suggested on the basis of the NMR data available at that time, consisted of two consecutive  $\beta$ -turns resulting in the formation of an incipient  $3_{10}$ -helical structure.<sup>[1a]</sup> In this structure, all the three residues must occupy the  $\alpha_R$  region of conformational space. No *cis* conformer was detected; leading to the conclusion that the Pro-Pro bond exclusively adopted a *trans* geometry. This finding was followed up by Kemp and co-workers<sup>[1c-e,9]</sup> who designed a synthetic template based on a diproline segment in which two pyrrolidine rings were covalently linked by a thiomethylene bridge. The success of Kemp's template in nucleating helix formation in

model peptide in aqueous solution is well documented.<sup>[1c-e]</sup> Hanessian successfully explored the development of synthetic diproline based organic templates in helix nucleation.<sup>[10]</sup> A recent study from our laboratory revisited the use of unconstrained diproline segments placed at the N-terminus of the model hexapeptide (Piv-L-Pro-L-Pro-Aib-Leu-Aib-Phe-OMe) in nucleating folded structures. While helix formation could be demonstrated over the segments 2 to 6, Pro(1) adopts a polyproline (P<sub>II</sub>) conformation in both crystals and in solution.<sup>[1b]</sup>

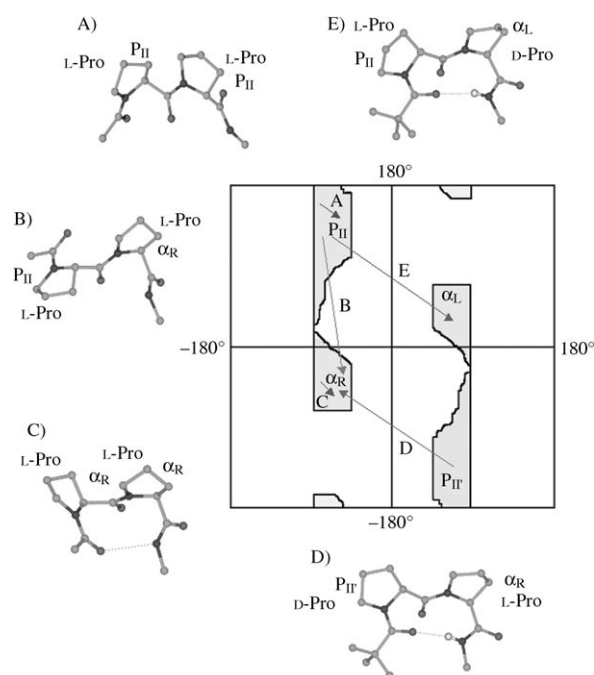


Figure 1. Ramachandran maps for D-Pro and L-Pro residues showing the available conformational space for proline. Arrows are used to roughly indicate the locations of the  $i+1$  and  $i+2$  residues in  $\phi, \psi$  space. The letters shown against the arrows indicate the diproline conformations. The possible conformation for diproline segments are indicated A) P<sub>II</sub>-P<sub>II</sub>, B) P<sub>II</sub>- $\alpha_R$ , C)  $\alpha_R$ - $\alpha_R$ , D) P<sub>II</sub>- $\alpha_R$ , E) P<sub>II</sub>- $\alpha_L$ . Note that the  $\alpha_R$ -P<sub>II</sub> combination is not observed in any diproline segment in the PDB.<sup>[1b]</sup>

The ability of D-Pro-Gly sequences to form type I/II'  $\beta$ -turns, provided the first successful approach to the design of stable, well characterized  $\beta$ -hairpin structures in short oligopeptides.<sup>[11]</sup> A large body of subsequent work has established the utility of centrally positioned D-Pro-Xxx sequences to facilitate sharp polypeptide chain reversal, thus facilitating the design of isolated  $\beta$ -hairpins<sup>[2b,4c,d,11e-h,12]</sup> and multi-stranded  $\beta$ -sheets.<sup>[2b,11h,13]</sup> The heterochiral D-Pro-L-Pro unit is an extremely efficient nucleator of  $\beta$ -hairpin structures since the segment has a marked propensity for type II'  $\beta$ -turn conformations.<sup>[14]</sup> Figure 2, illustrates the crystallographic characterization of a D-Pro-L-Pro segment as a nucleating unit in a synthetic hairpin and also provides an example of a L-Pro-L-Pro segment at the N-terminus of a helical segment in a protein.<sup>[15]</sup> Marshall and co-workers have suggested that L-Pro-L-Pro and D-Pro-D-Pro segments

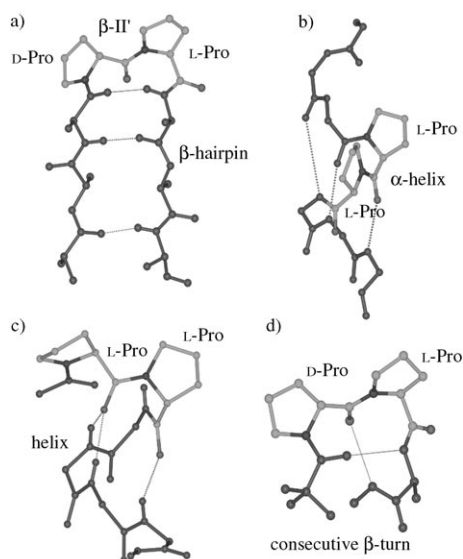


Figure 2. a)  $\beta$ -hairpin conformation of Piv-Leu-Phe-Val-D-Pro-L-Pro-Leu-Phe-Val-OMe in crystals,<sup>[2c]</sup> b) Pro-Pro segment in an  $\alpha$ -helix. PDB ID: 1QQF A (1250–1251),<sup>[15]</sup> c) Crystal state conformation of Piv-Pro-Pro-Aib-Leu-Aib-Phe-OMe,<sup>[1b]</sup> d) Consecutive  $\beta$ -turn conformation ( $\beta_{II-1}$ ) in the crystal structure of Piv-D-Pro-L-Pro-L-Ala-NHMe (DPPAN).<sup>[14]</sup>

are poor turn constraining units, due to enhanced *cis-trans* isomerism and small energy differences between turn-like and extended structures.<sup>[16]</sup> A recent study from this laboratory has demonstrated the ability of the D-Pro-L-Pro-D-Ala segment to form a three residue connecting loop in a well registered  $\beta$ -hairpin.<sup>[2c]</sup> Despite the widespread interest in diproline segments, systematic experimental investigations of model systems are lacking.

We present in this report conformational studies on 23 peptides containing diproline segments.<sup>[17]</sup> The crystal structures of 17 peptides (1–8, 10–15, 18, 20 and 23) designed to probe the allowed conformational space for both homochiral and heterochiral diproline units are presented. We also describe NMR studies, of some chosen sequences, to evaluate the occurrence of *cis* Pro-Pro conformations and the formation of type VI  $\beta$ -turns. The results demonstrate the importance of the C-terminus flanking residues as conformational determinants. The peptides examined are: Piv-D-Pro-L-Pro-NHMe (1); Piv-D-Pro-L-Pro-L-Xxx-OMe [L-Xxx = L-Val (2), L-Phe (3)]; Piv-D-Pro-L-Pro-D-Ala-OMe (4); Piv-L-Pro-D-Pro-L-Ala-OMe (5); Piv-D-Pro-L-Pro-L-Xxx-NHMe [L-Xxx = L-Val (6), L-Leu (7), L-Phe (8), Gly (9), Aib (10)]; Piv-D-Pro-L-Pro-D-Xxx-NHMe [D-Xxx = D-Ala (11), D-Val (12), D-Leu (13), D-Phe (14)]; Piv-L-Pro-D-Pro-L-Val-OMe (15); Piv-L-Pro-L-Pro-L-Xxx-OMe [L-Xxx = L-Ala (16), L-Val (17), L-Phe (18)]; Piv-L-Pro-L-Pro-L-Xxx-NHMe [L-Xxx = L-Ala (19), L-Val (20), L-Leu (21), L-Phe (22), Aib (23)].

The use of the Piv group at the N-terminus restricts the Piv-Pro tertiary amide bond to the *trans* conformation, a feature essential for the formation of  $\beta$ -turn structures with Pro(1) occupying the *i*+1 position.<sup>[1a,18]</sup>

## Results and Discussion

Attempts were made to obtain diffraction quality single crystals for all the peptides studied. Heterochiral diproline peptides appeared to crystallize more readily than their homochiral counterparts. In some cases, enantiomeric peptides were synthesized and recrystallization of peptide racemates was attempted. A brief report on the use of racemic mixtures in facilitating recrystallization and exploring multiple conformational states in proline peptides is presented elsewhere.<sup>[17]</sup> The backbone torsion angles in all the crystalline peptides and the relevant intramolecular hydrogen bonds are listed in Table 1. A complete list of hydrogen bond parameters for the crystal structures is provided as Supporting Information (Table S3).

### Crystal structures of D-Pro-L-Pro segments

**Type II'  $\beta$ -turns:** Figure 3 illustrates the molecular conformations observed in crystals of peptides 1–5. Peptide 1, Piv-D-Pro-L-Pro-NHMe is the prototypic, heterochiral diproline segment. The structure determination of 1 reveals two molecules in the asymmetric unit both of which adopt a type II'  $\beta$  turn conformation, with a single intramolecular 4 $\rightarrow$ 1 hydrogen bond between Piv C=O and NHMe (Table 1 and Supporting Information, Table S3). Similar conformations are observed in the tripeptide esters Piv-D-Pro-L-Pro-Xxx-OMe (Xxx=L-Val 2, L-Phe 3, D-Ala 4). Interestingly, the crystal structures of peptides 2 and 4 reveal multiple molecules in the asymmetric unit, three in the case of 2 and two in the case of 4. A structure determination of peptide 5, Piv-L-Pro-D-Pro-L-Ala-OMe yielded as anticipated, a type II  $\beta$ -turn structure (Figure 3e). The well-defined conformation of the heterochiral diproline segment is apparent when the eight independent molecules in the structure of peptides 1 to 4 are superposed yielding a RMSD value of 0.211 Å for the D-Pro-L-Pro segment.

**Consecutive  $\beta$ -turns:** Protected tripeptide N-methylamides of the type Piv-D-Pro-L-Pro-L-Xxx-NHMe fold into a consecutive  $\beta$ -turn ( $\beta_{II-1}$ ) conformation because of the presence of a donor NH group at the C-terminus which permits the formation of an additional 4 $\rightarrow$ 1 hydrogen bond. This structural feature was first characterized in Piv-D-Pro-L-Pro-L-Ala-NHMe in crystals<sup>[14]</sup> (Figure 2d). The conformations determined in crystals for peptides Piv-D-Pro-L-Pro-L-Val-NHMe (6), Piv-D-Pro-L-Pro-L-Leu-NHMe (7), Piv-D-Pro-L-Pro-L-Phe-NHMe (8) and Piv-D-Pro-L-Pro-Aib-NHMe (10) are illustrated in Figure 4. In all the cases, the molecules adopt the consecutive  $\beta$ -turn conformation ( $\beta_{II-1}$ ), with two intramolecular 4 $\rightarrow$ 1 hydrogen bonds (Table 1 and Table S3 in the Supporting Information). The superposition of the five independent molecules in Figure 4e with the parent Piv-D-Pro-L-Pro-L-Ala-NHMe establishes their close conformational similarity, with an RMSD of 0.387 Å.

Table 1. Torsion angles [°] and intramolecular hydrogen bonds.

Sequence	Residue 1 D-Pro/L-Pro			Residue 2 D-Pro/L-Pro			Residue 3			Intramolecular 4→1 Hydrogen bonds		
	$\phi$	$\psi$	$\omega$	$\phi$	$\psi$	$\omega$	$\phi$	$\psi$	$\omega$	Donor	Acceptor	N...O Distance [Å]
type II'/II $\beta$ -turns												
<b>1</b>												
molecule A	56.3	-139.2	178.4	-83.8	13.9	173.1	-	-	-	N(3)	O(0)	2.903
molecule B	57.7	-134.7	179.9	-81.5	5.3	175.3	-	-	-	N(6)	O(3)	2.926
<b>2</b>												
molecule A	61.5	-133.2	180.0	-73.2	-7.3	-175.8	-115.5	177.6	178.3	N(3)	O(0)	3.013
molecule B	60.5	-138.1	-177.6	-87.4	14.1	-180.0	-95.6	-46.6	-175.5	N(7)	O(4)	3.122
molecule C	59.5	-139.4	-179.8	-80.4	-4.4	-175.3	-72.5	135.6	176.8	N(11)	O(8)	3.033
<b>3</b>	59.8	-137.6	-178.1	-81.4	0.7	-179.2	-83.5	177.2	-173.4	N(3)	O(0)	3.052
<b>4</b>												
molecule A	57.6	-144.7	-179.7	-82.9	-0.6	-178.5	55.9	-139.4	178.0	N(3)	O(0)	3.095
molecule B	57.0	-143.3	-179.0	-82.8	0.7	-175.2	63.4	-149.9	-175.1	N(6)	O(00)	3.114
<b>5</b>	-64.8	137.3	177.8	85.3	-6.1	176.0	-68.9	160.4	176.2	N(3)	O(0)	3.147
consecutive $\beta$ -turns												
<b>6</b>	57.0	-135.3	-170.9	-72.7	-4.6	175.8	-116.8	17.5	172.5	N(3) N(4)	O(0) O(1)	3.168 3.148
<b>7</b>												
molecule A	65.0	-135.7	-178.8	-69.3	-6.7	172.2	-92.7	4.3	177.3	N(3) N(4)	O(0) O(1)	3.024 2.974
molecule B	56.9	-141.7	-178.9	-68.3	-9.5	174.9	-85.1	-6.6	177.3	N(7) N(8)	O(4) O(5)	3.051 3.019
<b>8</b>	62.1	-141.0	-175.2	-68.3	-12.3	176.7	-75.5	-17.9	-179.9	N(3) N(4)	O(0) O(1)	3.144 3.109
<b>10</b>	59.5	-153.6	177.7	-75.2	-16.0	179.4	-60.2	-35.7	-177.5	N(3) N(4)	O(0) O(1)	3.262 3.445
effect of residue 3 <sup>[b]</sup>												
<b>11</b> <sup>[a]</sup>	60.7	-153.5	-180.0	-85.7	30.5	168.8	129.4	34.1	175.3	N(3)	O(0)	3.291
<b>12</b>	66.4	-141.2	8.4	-78.1	158.5	170.8	77.7	-159.2	-176.8	-	-	-
							94.1	-167.5	-179.9			
<b>13</b> <sup>[17]</sup>	68.5	-165.5	-178.4	-64.8	137.7	-178.4	89.6	-2.7	-178.4	N(4)	O(1)	3.184
<b>14</b> <sup>[17]</sup>	63.9	-141.0	12.6	-76.9	139.5	168.9	118.7	-151.8	-175.7	-	-	-
<b>15</b>	-62.8	143.0	-9.4	78.1	-153.0	-169.9	-87.1	169.4	176.8	-	-	-
homochiral L-Pro-L-Pro sequences												
<b>18</b>												
molecule A	-54.5	141.4	11.0	-88.5	2.9	177.6	-74.4	-156.3	177.9	N(3)	O(0)	2.865
molecule B	-52.4	141.4	7.5	-90.8	8.1	168.3	-74.8	-3.1	-177.2	N(7)	O(4)	2.857
<b>20</b>	-75.3	137.4	170.5	-63.5	-30.5	-175.7	-135.5	116.0	-179.2	-	-	-
<b>23</b>	-95.9	173.3	168.8	-57.1	136.4	174.1	57.1	34.5	172.8	N(4)	O(1)	3.273

[a] In addition to the 4→1 interaction there is also 5→1 intramolecular hydrogen bond between N(4) and O(0) with a N...O distance of 2.849 Å.

[b] Effect on the configuration of D-Pro-L-Pro segment.

### Effect of residue 3 configuration on D-Pro-L-Pro conformations:

Figure 5a shows the molecular conformation of Piv-D-Pro-L-Pro-D-Ala-NHMe (**11**). The D-Pro(1)-L-Pro(2) segment in this structure forms a type II'  $\beta$ -turn conformation as anticipated, with a 4→1 ( $C_{10}$ ) hydrogen bond between the Piv C=O and D-Ala(3) NH groups. The D-Ala residue adopts an unusual conformation ( $\phi = 129.4$ ,  $\psi = 34.1^\circ$ ), which lies in the sterically allowed region of  $\phi, \psi$  space. This results in the formation of a strong 5→1 intramolecular hydrogen bond between the Piv C=O and methylamide NH groups (N...O = 2.849 Å). Consideration of the structure of the peptide suggests that although the Piv C=O group participates in bifurcated interactions with two hydrogen bond donors, the dominant interaction is of the 5→1 ( $C_{13}$ ) type. Such structures have been observed in proteins and are classified as  $\alpha$ -turns.<sup>[19]</sup> Isolated  $\alpha$ -turn structures have thus far not been observed in crystal structures of short peptides and

peptide **11** provides the first example of such a conformational feature. An enantiomeric peptide Piv-L-Pro-D-Pro-L-Ala-NHMe was synthesized and yielded single crystals with identical cell dimensions suggesting an identity of molecular conformation. The structure of peptide **11** may be compared with the methyl ester analog Piv-D-Pro-L-Pro-D-Ala-OMe (**5**) in which a single D-Pro(1)-L-Pro(2) type II'  $\beta$ -turn is observed. Clearly, the additional hydrogen bond donor in peptide **11** is an important conformational determinant.

The peptide Piv-D-Pro-L-Pro-D-Val-NHMe<sup>[17]</sup> (**12**) provides an example of an unusual conformation in which the D-Pro-L-Pro peptide bond adopts a *cis* geometry, with the absence of any intramolecular hydrogen bonding interaction (Figure 5b). Surprisingly, the enantiomeric peptide Piv-L-Pro-D-Pro-L-Val-NHMe<sup>[17]</sup> reveals the expected type II  $\beta$ -turn conformation at the L-Pro-D-Pro segment (Figure 5c). Undoubtedly, the hydration of central peptide unit observed

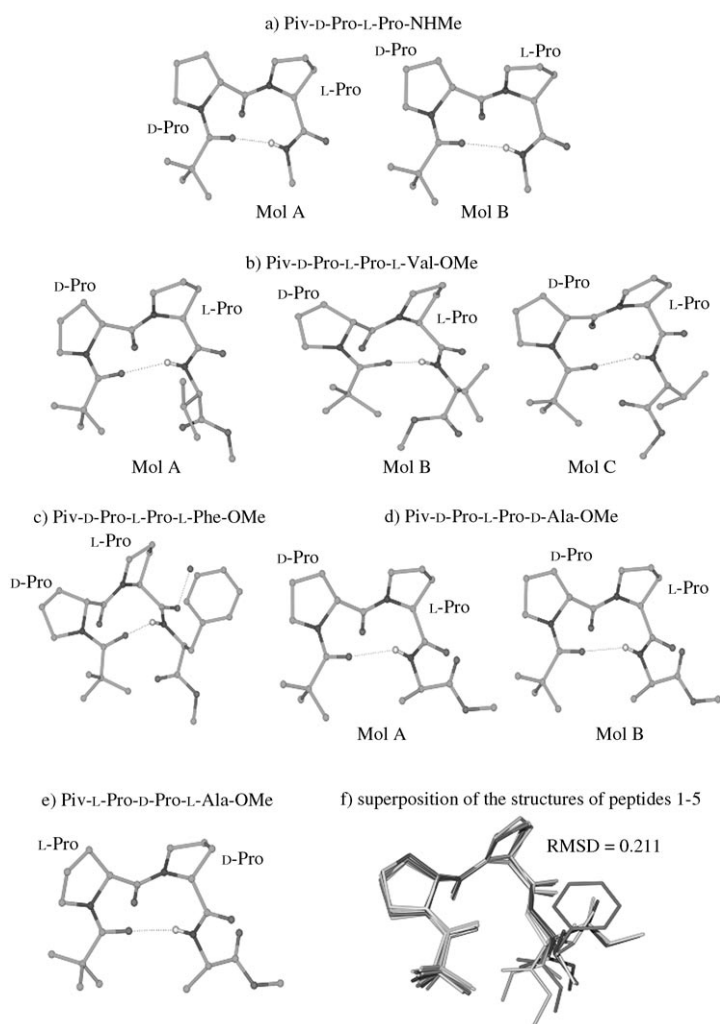


Figure 3. Molecular conformation of peptides in crystals containing heterochiral diproline segments a) Piv-D-Pro-L-Pro-NHMe (**1**), b) Piv-D-Pro-L-Pro-L-Val-OMe (**2**), c) Piv-D-Pro-L-Pro-L-Phe-OMe (**3**), d) Piv-D-Pro-L-Pro-D-Ala-OMe (**4**), e) Piv-L-Pro-D-Pro-L-Ala-OMe (**5**), f) superposition of the structures of peptides 1–5.

in the D-L-D peptide **12**, result in an unfolded backbone conformation. In order to evaluate the role of terminal methylamide NHMe group, the crystal structure of the corresponding tripeptide ester Piv-L-Pro-D-Pro-L-Val-OMe (**15**) was solved. The molecular conformation shown in Figure 5d reveals a *cis* L-Pro-D-Pro bond with the absence of any intramolecular hydrogen bond. This conformation is remarkably similar to that observed in the tripeptide (Piv-D-Pro-L-Pro-D-Val-NHMe). The crystal structure determination of a crystalline racemate containing both the L-D-L and the D-L-D peptides revealed only the type II/II'  $\beta$ -turn conformation with the enantiomeric molecules related by inversion symmetry.<sup>[17]</sup> These observations suggest that the multiple conformational states that exist in solution may crystallize preferentially under specific conditions. Interestingly, the crystal structure of the peptide Piv-D-Pro-L-Pro-D-Leu-NHMe<sup>[17]</sup> (**13**) does not show the anticipated D-Pro-L-Pro type II'  $\beta$ -

turn (Figure 5e). Instead, the L-Pro-D-Leu segment adopts a type II  $\beta$ -turn conformation with D-Pro(1) taking up a D-Pro<sub>II</sub> conformation ( $\phi=68.8^\circ$ ,  $\psi=-167.5^\circ$ ). Notably, in the D-Pro-L-Pro-D-Xxx-NHMe series, completely distinct conformers have been characterized for D-Xxx = D-Ala, D-Val and D-Leu. In contrast, in the case of D-Pro-L-Pro-L-Xxx-NHMe series, all the peptides studied (L-Xxx = L-Ala, L-Val, L-Phe, L-Leu and Aib) yielded the same conformation in crystals. In attempting to obtain suitable single crystals for X-ray diffraction studies, we have investigated the utility of racemic mixtures formed by using equimolar amounts of pure peptide enantiomers. The crystal structures of three racemic peptides in which the residue configurations alternate (D-L-D/L-D-L) that have been discussed elsewhere may provide a means of exploring polymorphic forms in which multiple conformational states may be definitively characterized.<sup>[17]</sup> Notably, for the racemic mixture involving L/D-Phe<sup>[17]</sup> (**14**), the asymmetric unit contains a single peptide molecule, which adopts an open structure lacking any intramolecular hydrogen bond (Figure 5f).

**Homochiral L-Pro-L-Pro sequences:** The structures of three independent peptides Piv-L-Pro-L-Pro-L-Phe-OMe (**18**), Piv-L-Pro-L-Pro-L-Val-NHMe (**20**) and Piv-L-Pro-L-Pro-Aib-NHMe (**23**) are shown in Figure 6. In peptide **18**, both molecules in the crystallographic asymmetric unit adopt a type VIa  $\beta$ -turn conformation<sup>[3c,4b,20]</sup> ( $\phi_{i+1}=-60^\circ$ ,  $\psi_{i+1}=120^\circ$ ;  $\phi_{i+2}=-90^\circ$ ,  $\psi_{i+2}=0^\circ$ ), in which the L-Pro-L-Pro peptide bond is *cis* ( $\omega=11.0^\circ$  in the case of molecule A and  $7.5^\circ$  in the case of molecule B). A 4 $\rightarrow$ 1 hydrogen bond between the Piv C=O and the Phe(3) NH is observed (Table 1 and Supporting Information, Table S3). A similar conformation has been characterized in the peptide ferrocenyl-Pro-Pro-Phe-OBzl.<sup>[21]</sup> Interestingly, earlier studies on small linear peptides and protein structures have revealed a tendency for the Xaa-Pro peptide bond to adopt a *cis* geometry when the proline residue is preceded by an aromatic residue.<sup>[22]</sup> A structure devoid of any intramolecular hydrogen bonds is observed in peptide **20**. Pro(1) adopts a P<sub>II</sub> conformation with Pro(2) lying in the helical  $\alpha_R$  region and Val(3) in the extended  $\beta$ -sheet region. In peptide **23**, a Pro(2)-Aib(3) type II  $\beta$ -turn is observed with a 4 $\rightarrow$ 1 intramolecular hydrogen bond between Pro(1) C=O and the methylamide NH group. Pro(1) adopts a conformation which is considerably distorted from that observed for proline residues ( $\phi=-95.9^\circ$ ,  $\psi=173.3^\circ$ ). In this case the Pro(1) ring exhibits an unusual puckering ( $\chi_1=37.8^\circ$ ,  $\chi_2=-33.9^\circ$ ,  $\chi_3=17.0^\circ$ ,  $\chi_4=7.5^\circ$ ,  $\theta=-28.5^\circ$  for the first proline ring and  $\chi_1=-22.4^\circ$ ,  $\chi_2=35.6^\circ$ ,  $\chi_3=-34.5^\circ$ ,  $\chi_4=21.2^\circ$ ,  $\theta=0.6^\circ$  for the second proline ring). Notably, in all the three cases of homochiral tripeptides **18**, **20** and **23** a water of hydration is observed in the crystals. This lone water molecule is hydrogen bonded to the Pro(1) C=O group in all the three peptides. In the case of peptide **18**, the asymmetric unit contains two molecules of the peptide and only one molecule of water. In peptide **20**, the water molecule interacts with both the free NH groups of Val(3) and the methylamide group. In peptide **23**, the intra-

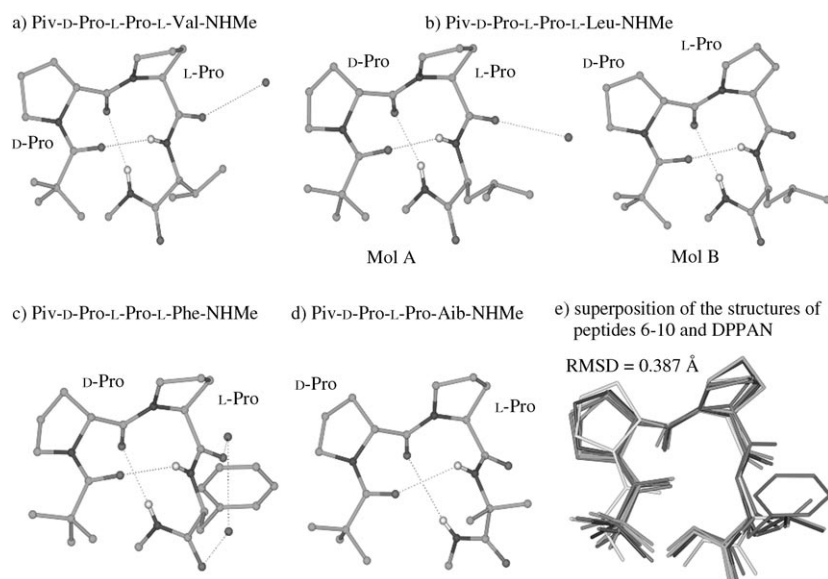


Figure 4. Molecular conformation of peptides in crystals containing consecutive  $\beta$ -turns a) Piv-D-Pro-L-Pro-L-Val-NHMe (**6**), b) Piv-D-Pro-L-Pro-L-Leu-NHMe (**7**), c) Piv-D-Pro-L-Pro-L-Phe-NHMe (**8**), d) Piv-D-Pro-L-Pro-Aib-NHMe (**10**), e) superposition of the structures of peptides **6–10** and DPPAN.

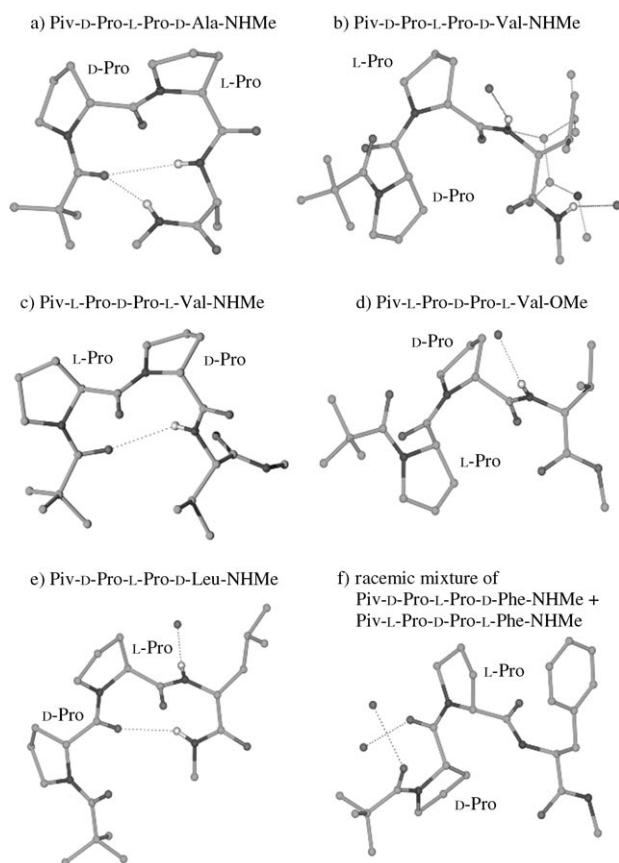


Figure 5. Molecular conformation of peptides in crystals containing a D-residue succeeding the heterochiral diproline segments a) Piv-D-Pro-L-Pro-D-Ala-NHMe (**11**), b) Piv-D-Pro-L-Pro-D-Val-NHMe (**12**),<sup>[17]</sup> c) Piv-L-Pro-D-Pro-L-Val-NHMe,<sup>[17]</sup> d) Piv-L-Pro-D-Pro-L-Val-OMe (**15**), e) Piv-D-Pro-L-Pro-D-Leu-NHMe,<sup>[17]</sup> (**13**), f) racemic mixture of Piv-D-Pro-L-Pro-D-Phe-NHMe + Piv-L-Pro-D-Pro-L-Phe-NHMe<sup>[17]</sup> (**14**). Only the D-L-D enantiomer has been shown.

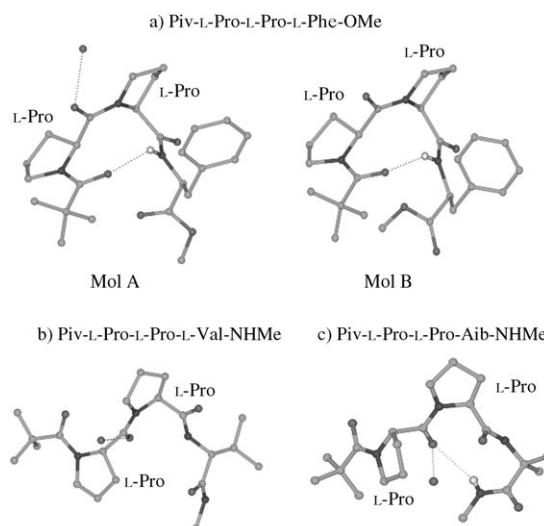


Figure 6. Molecular conformation of peptides in crystals containing homochiral diproline segments a) Piv-L-Pro-L-Pro-L-Phe-OMe (**18**), b) Piv-L-Pro-L-Pro-L-Val-NHMe (**20**), c) Piv-L-Pro-L-Pro-Aib-NHMe (**23**).

molecular  $\beta$ -turn hydrogen bond appears weak with a N $\cdots$ O distance of 3.273 Å, presumably as a consequence of a strong bifurcated interaction of Pro(1) C=O with the hydrating water molecule.

**Conformations of the proline ring:** The puckering of the five-membered pyrrolidine ring in proline residues has been the subject of investigation for almost four decades.<sup>[23g]</sup> Important studies which define proline ring conformations merit mention. In 1970 Ramachandran and co-workers<sup>[23a]</sup> established two major conformational states which describe the relative positions of the C $\gamma$  and the C' atoms with respect to the mean plane formed by the

other four atoms of the five-membered ring as A (C $\gamma$ /C' atoms on opposite side, C $\gamma$ -*exo*) and B (C $\gamma$ /C' atoms on same side, C $\gamma$ -*endo*). Subsequently, an incisive study by Ashida and Kakudo<sup>[23b]</sup> described C $_s$ -C $\gamma$ -*exo*, C $_s$ -C $\gamma$ -*endo*, C $_s$ -C $^\beta$ -*exo*, C $_s$ -C $^\beta$ -*endo*, C $_2$ -C $\gamma$ -*exo*-C $_2$ -C $^\beta$ -*endo* and C $_2$ -C $\gamma$ -*endo*-C $_2$ -C $^\beta$ -*exo*. In an important contribution Scheraga and co-workers<sup>[23c,d]</sup> defined these states using the nomenclature up and down. A generalized description of five-membered ring conformations introduced by Cremer and Pople<sup>[23e]</sup> which uses two parameters (the amplitude  $q$  and the phase angle  $\phi$ ) has sometimes been used for the description of the proline ring.

A study published in 1977 by De Tar and Luthra<sup>[23f]</sup> effectively identified two major states of the proline ring. More recent theoretical<sup>[23h]</sup> and database analysis<sup>[23i,j]</sup> studies have focused on an analysis of the coupling between the proline ring geometry and the polypeptide backbone. While many descriptions of ring geometry have been advanced, it is convenient to adopt a classification scheme which is based on endocyclic torsion angles since these readily permit visualization of the distortions of the five-membered pyrrolidine ring from planarity. The availability of a large number of structurally characterized diproline segments in the present study prompted us to revisit the analysis of the proline ring geometry. In particular, most observed forms of the proline ring are simply visualized by considering the  $C^\alpha$ -N- $C^\delta$  plane as a reference and describing the positions of the  $C^\beta$  and the  $C^\gamma$  atoms with respect to this plane. For example, values of  $\chi_4$  close to zero immediately indicate that the  $C^\gamma$  atom lies in the plane and that the puckering must be localized at  $C^\beta$ . Similarly, a value of  $\theta$  close to zero is an indicator of  $C^\gamma$  puckering with the  $C^\beta$  atom lying in the plane. Cases where both  $\chi_4$  and  $\theta$  are greater than  $10^\circ$  are immediately diagnostic of twisted proline geometry, in which both  $C^\beta$  and  $C^\gamma$  atoms lie out of plane. A few cases are also observed where  $\chi_4 \sim \theta \sim 0^\circ$ , which corresponds to an almost flattened, nearly planar ring conformation.

Peptide crystal structures, determined at atomic resolution provide a wealth of data on proline rings. Table 2 summarizes the observations on proline rings in diproline segments characterized crystallographically. A total of 44 diproline segments have been examined in acyclic compounds out of which 21 have been extracted from the Cambridge Crystallographic Database.<sup>[24]</sup> The classification of ring conformations in individual residues and in diproline segments are given as Supporting Information (Tables S4–S6). Investigation of the ring conformations reveals six distinct conformational states. Two states which are maximally populated correspond to displacement of only one of the ring atoms from the mean plane, that is,  $C_s$ - $C^\gamma$ -*exo*(19) and  $C_s$ - $C^\beta$ -*exo*(21). Significant populations of four more states are also noted. These are  $C_s$ - $C^\gamma$ -*endo*, two twisted states in which both the  $C^\gamma$  and the  $C^\beta$  atoms are move out of the plane and a near planar geometry of the five-membered ring. Significantly, an almost planar five-membered ring is observed in as many as 13 out of 88 proline rings. Indeed a planar proline ring has also been characterized in a high resolution structure of the protein, triosephosphate isomerase.<sup>[25]</sup> Interestingly, there is no example of a state which can be characterized as  $C_s$ - $C^\beta$ -*endo*. Examination of the conformations of proline rings in diproline segments does not reveal any dramatic preference for a specific state, in the case of homochiral segments. However, in the case of heterochiral diproline segments there is a preponderance of the  $C^\gamma$ -*exo*/ $C^\beta$ -*exo* combination. Figure 7 illustrates the six major classes of observed ring conformational states. It is necessary to draw attention to the structure of Boc-Pro-Pro-OH (CSD ID-BOCPRO01) in which four independent dipeptide molecules constitute the crystallographic asymmetric unit. While molecules 3 and 4

have been taken into the dataset for the preceding analysis, molecules 1 and 2 are considered separately. In this case, the following ring torsion angles are observed [molecule 1: Pro(1):  $\chi_1=25.8^\circ$ ,  $\chi_2=-34.4^\circ$ ,  $\chi_3=29.7^\circ$ ,  $\chi_4=-13.3^\circ$ ,  $\theta=-7.5^\circ$ , Pro(2):  $\chi_1=24.6^\circ$ ,  $\chi_2=-15.2^\circ$ ,  $\chi_3=0.0^\circ$ ,  $\chi_4=16.6^\circ$ ,  $\theta=-25.8^\circ$ ; molecule 2: Pro(1):  $\chi_1=26.3^\circ$ ,  $\chi_2=-33.8^\circ$ ,  $\chi_3=27.1^\circ$ ,  $\chi_4=-10.3^\circ$ ,  $\theta=-9.7^\circ$ , Pro(2):  $\chi_1=24.1^\circ$ ,  $\chi_2=-13.9^\circ$ ,  $\chi_3=0.2^\circ$ ,  $\chi_4=14.4^\circ$ ,  $\theta=-21.9^\circ$ ]. In both the molecules Pro(1) is classified as twisted  $C^\gamma$ -*endo*. However, Pro(2) in both the cases has a  $\chi_3 \sim 0^\circ$  which is directly indicative of the fact that the atoms N- $C^\delta$ - $C^\gamma$  and  $C^\beta$  lie in a plane with the ring being distorted by the movement of  $C^\alpha$  atom out of the plane (Figure 7). This is a rare example of a geometry which arises from puckering at  $C^\alpha$ . The pyrrolidine ring conformations within diproline segments do not show a strong co-relation to the backbone structural feature in which they are found. It is likely that five membered rings have a considerable plasticity of structure and are readily deformed in order to accommodate a variety of energetically preferred backbone conformations.

#### Solution conformations of peptides with diproline segments:

Crystallographic studies, described in the preceding section, establish distinct conformational preferences in model peptides containing D-Pro-L-Pro and L-Pro-L-Pro sequences. An important feature to emerge from these studies is that conformational diversity is observed in the solid state, especially in the case of D-Pro-L-Pro-D-Xxx and L-Pro-L-Pro-L-Xxx sequences, suggesting that in solution, multiple conformational states are almost certainly likely to be populated. NMR studies have therefore, been undertaken in order to probe the nature of the conformations populated in solution, in organic solvents. The existence of hydrogen bonded conformations have been probed using solvent dependence of amide NH chemical shifts, while specific nuclear Overhauser effects (NOEs) are used as a diagnostic for determining local residue conformations.

**Heterochiral D-Pro-L-Pro sequences:** Table 3 lists the observed chemical shift for the two amide protons and the values for the change in chemical shift on going from pure  $CDCl_3$  to a mixture containing an appreciable concentration of high [ $D_6$ ]DMSO (21.7% v/v). The addition of varying concentrations of the strongly hydrogen-bonded solvent DMSO to the peptides in the poorly interacting solvent,  $CDCl_3$  is expected to cause a large downfield shift of the solvent exposed protons as a consequence of the interaction with the added solvent. Inspection of  $\Delta\delta$  values listed in Table 3 clearly reveals that in the D-Pro-L-Pro-L-Xxx series, where L-Xxx = L-Val (6), L-Leu (7), L-Phe (8), Gly (9), Aib (10), the  $\Delta\delta$  values are exceedingly small (0.02 to 0.11 ppm). This strongly suggests that both the NH groups are solvent shielded, supporting their involvement in strong intramolecular hydrogen bonding. These results suggest that the consecutive type II'-I  $\beta$ -turn structures observed in crystals of 6, 7, 8 and 10 are indeed maintained in solution. NOE studies of the peptide Piv-D-Pro-L-Pro-L-Phe-NHMe (8), reveals in-



Table 2. Puckering states of the proline ring.

Ring conformation	Number of proline rings <sup>[a]</sup>	Average ring torsional parameters [°]	Combination	No. of examples in homochiral diproline segments <sup>[a]</sup>	No. of examples in heterochiral diproline segments <sup>[a]</sup>
A) <i>C<sub>s</sub></i> - <i>C<sup>γ</sup></i> - <i>exo</i> or <i>C<sup>γ</sup></i> - <i>exo</i>	8 + <b>11</b> = 19	$\chi_1 = -20.4, \chi_2 = 32.9, \chi_3 = -32.0,$ $\chi_4 = 19.5, \theta = 0.4$	AC BB AG	<b>2</b> – –	4 + <b>1</b> 2 1 + <b>1</b>
B) <i>C<sub>s</sub></i> - <i>C<sup>γ</sup></i> - <i>endo</i> or <i>C<sup>γ</sup></i> - <i>endo</i>	7 + <b>1</b> = 8	$\chi_1 = 22.6, \chi_2 = -33.1, \chi_3 = 30.2,$ $\chi_4 = -16.0, \theta = -4.0$	GC BC BF GF EC	<b>1</b> – – <b>3</b> 2 + <b>1</b>	1 1 2 2 <b>1</b>
C) <i>C<sub>s</sub></i> - <i>C<sup>β</sup></i> - <i>exo</i>	11 + <b>10</b> = 21	$\chi_1 = 34.1, \chi_2 = -36.7, \chi_3 = 24.3,$ $\chi_4 = -2.2, \theta = -20.1$	GE AF FC	1 – –	– 2 2 + 1
D) <i>C<sub>s</sub></i> - <i>C<sup>β</sup></i> - <i>endo</i>	–	–	AB CC	<b>1</b> <b>1</b>	– –
E) twisted <i>C<sup>γ</sup></i> - <i>exo</i> - <i>C<sup>β</sup></i> - <i>endo</i> or <i>C<sub>2</sub></i> - <i>C<sup>γ</sup></i> - <i>exo</i> - <i>C<sub>2</sub></i> - <i>C<sup>β</sup></i> - <i>endo</i>	5 + <b>5</b> = 10	$\chi_1 = -29.7, \chi_2 = 38.7, \chi_3 = -32.2,$ $\chi_4 = 13.9, \theta = 9.8$	FA AE FF AA	<b>1</b> <b>3</b> <b>1</b> –	– – – 1
F) twisted <i>C<sup>γ</sup></i> - <i>endo</i> - <i>C<sup>β</sup></i> - <i>exo</i> or <i>C<sub>2</sub></i> - <i>C<sup>γ</sup></i> - <i>endo</i> - <i>C<sub>2</sub></i> - <i>C<sup>β</sup></i> - <i>exo</i>	9 + <b>8</b> = 17	$\chi_1 = 30.5, \chi_2 = -38.1, \chi_3 = 30.4,$ $\chi_4 = -11.6, \theta = -11.7$	FC GG EF EG	<b>1</b> <b>1</b> – –	– – 1 1
G) planar	6 + <b>7</b> = 13	$\chi_1 = 6.2, \chi_2 = -5.1, \chi_3 = 1.7,$ $\chi_4 = 2.6, \theta = -5.5$	CA	1	–

[a] Numbers highlighted in bold font are examples from CSD.

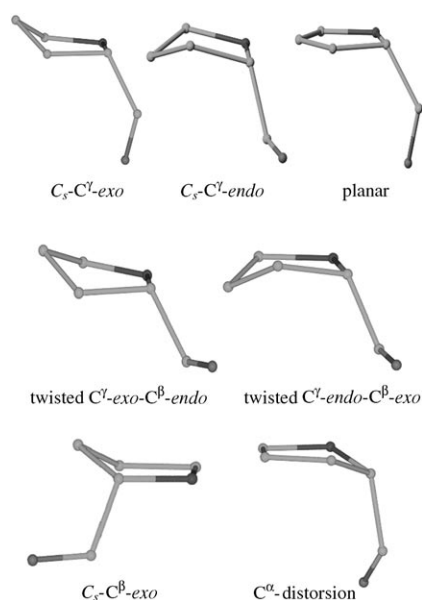


Figure 7. Puckering states of proline rings.

tense NOEs between Pro(1) C<sup>α</sup>H⇌Pro(2)C<sup>δ</sup>H confirming the *trans* geometry about the Pro(1)-Pro(2) bond. Further,

the Pro(2)C<sup>α</sup>H⇌Phe(3)NH and Phe(3)NH⇌NHMe NOEs are consistent with β-turn conformations.

Interestingly, in the case of the D-Pro-L-Pro-D-XXX-NHMe series, the Δδ values observed for D-XXX NH are extremely small (–0.06 to 0.10 ppm), while the values for methylamide NH are appreciably larger (0.26 to 0.36 ppm) indicative of a greater degree of solvent exposure of the C-terminal amide.

Table 3. NMR parameters for the peptides Piv-D-Pro-L-Pro-L-XXX-NHMe and Piv-D-Pro-L-Pro-D-XXX-NHMe.

Residues Xxx	Chemical shift [ppm] <sup>[a]</sup>		Δδ [ppm] <sup>[b]</sup>	
	Xxx	NH NHMe	Xxx	NHMe
Piv-D-Pro-L-Pro-L-XXX-NHMe				
Gly ( <b>9</b> )	7.84	7.01	0.06	0.11
Aib ( <b>10</b> )	6.85	6.96	0.02	0.05
L-Val ( <b>6</b> )	6.99	6.76	0.04	0.08
L-Leu ( <b>7</b> )	7.25	6.91	0.06	0.07
L-Phe( <b>8</b> )	7.38	6.85	0.04	0.08
Piv-D-Pro-L-Pro-D-XXX-NHMe				
D-Ala ( <b>11</b> )	7.52	7.01	0.03	0.27
D-Val ( <b>12</b> )	7.62	7.02	–0.04	0.28
D-Leu ( <b>13</b> )	7.48	7.11	0.04	0.26
D-Phe( <b>14</b> )	7.46	6.99	0.08	0.28

[a] CDCl<sub>3</sub>. [b] Δδ is chemical shift difference for NH protons in CDCl<sub>3</sub> and 21.7% [D<sub>6</sub>]DMSO/CDCl<sub>3</sub> (v/v) solutions.



Significantly, the crystal structure determination of the three members of this group D-Xxx = D-Ala (**11**), D-Val (**12**), D-Leu (**13**) revealed three distinct structures. In the case of the peptide D-Xxx = D-Ala (**11**), both the amide NH groups are involved in intramolecular hydrogen bonding. But in the case of D-Xxx = D-Val (**12**), neither of the amide NH(s) were hydrogen bonded, while in D-Xxx = D-Leu (**13**), a single intramolecular hydrogen bond involving a methyl amide NH group was observed. The NMR results suggest that in solution, the D-Pro-L-Pro  $\beta$ -turn is stabilized by a 4  $\rightarrow$  1 hydrogen bond between Piv C=O and D-Xxx NH group and is maintained in all the cases with a degree of conformational variability involving the C-terminal residue. Notably, in the three crystal structures which have been determined in this series the D-Xxx, D-Ala residue, adopts a conformation of ( $\phi=129^\circ$  and  $\psi=34^\circ$ ) in the relatively unpopulated, but nevertheless allowed, regions of the Ramachandran map. In contrast, the D-Leu residue in peptide **13**, adopts an  $\alpha_L$  conformation, while the D-Val residue in peptide **12** adopts an extended conformation, ( $\phi \sim 90\text{--}110^\circ$  and  $\psi \sim 140\text{--}160^\circ$ ), in two distinct structures observed in pure enantiomers and racemic mixtures. Thus, the heterogeneity of the conformations in the D-Pro-L-Pro-D-Xxx-NHMe series involving residue 3 observed in the crystalline state undoubtedly manifests itself also in solution, as evidenced by moderately high  $\Delta\delta$  values, observed in the solvent titration experiments. NOE studies in the D-Pro-L-Pro-D-Xxx-NHMe series of the peptides revealed strong Pro(1) C <sup>$\alpha$</sup> H–Pro(2) C <sup>$\delta$</sup> H NOEs, confirming that the Pro(1)–Pro(2) bond is predominantly *trans*. Indeed, there is little evidence for the presence of a minor *cis* conformation in all the peptides studied. Curiously, the structure of the pure enantiomer, Piv-D-Pro-L-Pro-D-Val-NHMe

(**12**) determined in single crystals obtained from the mixture of an ethyl acetate and petroleum ether reveals a *cis* Pro(1)–Pro(2) peptide bond in the crystalline state. In peptides **11** and **12**, relatively intense NOEs were observed between Pro(2) C <sup>$\delta$</sup> H $\rightleftharpoons$ Xxx NH, Pro(2) C <sup>$\alpha$</sup> H $\rightleftharpoons$  Xxx NH and Xxx NH $\rightleftharpoons$ NHMe. The simultaneous observation of these NOEs is a clear indication of the population of multiple conformational states in solution. While the D-Pro-L-Pro sequence appears to have a strong propensity for forming type II'  $\beta$ -turns, the Pro(2)-D-Xxx(3) segment is less constrained, with the nature of D-Xxx residue being a determining feature.

**Homochiral L-Pro-L-Pro sequences:** The delineation of solvent shielded NH groups was carried out by monitoring the downfield shift of NH resonances upon addition of strongly hydrogen bonded solvent [ $D_6$ ]DMSO to the peptide solution in  $CDCl_3$ . Representative solvent titration curves are shown in the Figure 8. The population of *cis* conformer about Pro–Pro bond was evident in all the sequences by the appearances of additional resonances. The assignment of the resonances of the *cis* form is based on the observation of a NOE between Pro(1) and Pro(2) C <sup>$\alpha$</sup> H protons. Further, HSQC ( $^1H\text{--}^{13}C$ ) spectra of peptides **19** and **22**, permitted the assignment of C <sup>$\beta$</sup>  and C <sup>$\gamma$</sup>  carbon resonances. In the case of the *cis* conformer of peptide **22**, the C <sup>$\beta$</sup>  resonances of Pro(2) appears at 31.6 ppm while C <sup>$\gamma$</sup>  resonances appear at 21.2 ppm. In contrast, *trans* form of peptide 19, the C <sup>$\beta$</sup>  chemical shift of Pro(2) is at 29.3 ppm while C <sup>$\gamma$</sup>  appears at 24.2 ppm (see Supporting Information, Table S7). A large  $\Delta\delta$  (C <sup>$\beta$</sup> –C <sup>$\gamma$</sup> ) of  $\sim 10$  ppm is characteristic of a *cis* X-Pro bond.<sup>[26]</sup> Table 4 summarizes the  $^1H$  NMR parameters determined for the series of peptides Piv-L-Pro-L-Pro-L-Xxx-NHMe/OMe. In a study of L-Xxx = L-Ala peptide (**19**) published over 25 years ago, two strongly hydrogen bonded NH groups were identified and the consecutive type III–III  $\beta$ -turn conformation was assigned. Reinvestigation of this peptide, synthesized afresh, revealed that both NH groups are involved in intramolecular hydrogen bonding. Furthermore, the NMR spectrum revealed an overwhelming presence of *trans* conformer, now conclusively established by the Pro(1)C <sup>$\alpha$</sup> H  $\rightleftharpoons$  Pro(2)C <sup>$\delta$</sup> H NOEs. Careful examination of the spectrum reveals that the *cis* conformer is populated to an extent of 5%. Interestingly, in all other peptides in these series, a significantly higher proportion of *cis* conformer was observed.

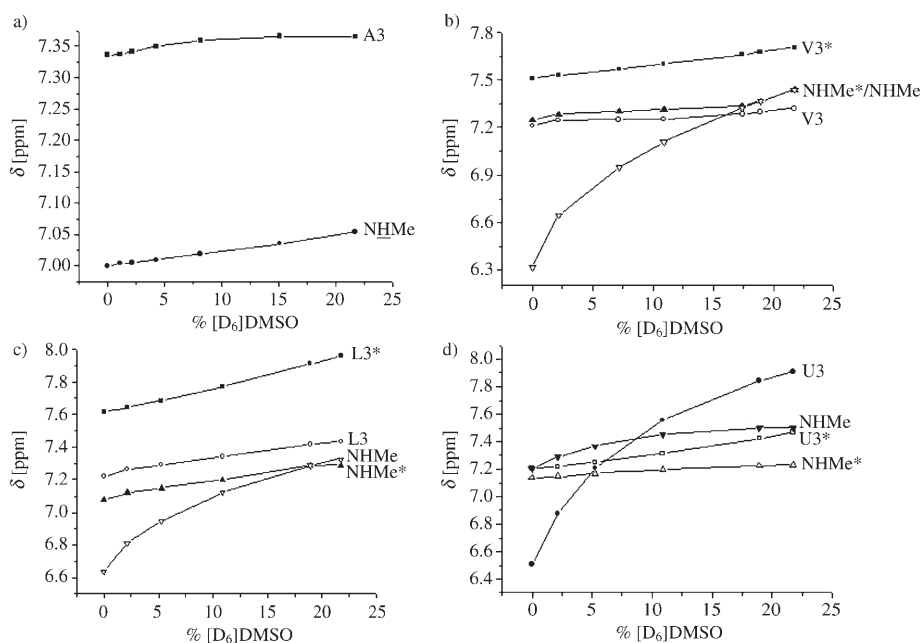


Figure 8. Representative experiments showing the solvent dependence of NH chemical shifts at varying concentrations of [ $D_6$ ]DMSO in  $CDCl_3$  to probe solvent exposed versus hydrogen bonded amides. \* Corresponds to *cis* conformation. a) **19**, b) **20**, c) **21**, d) **23**.

Table 4. NMR parameters for the peptides Piv-L-Pro-L-Pro-L-Xxx-NHMe/OMe in CDCl<sub>3</sub> and [D<sub>6</sub>]DMSO<sup>[a]</sup> solutions.

Residues (L-Xxx)	Conformers	Chemical shift [ppm]		Δδ [ppm] <sup>[b]</sup>		<i>cis</i> [%]	Δ <i>G</i> <sup>[c]</sup> <sub><i>cis/trans</i></sub>
		Xxx	NHMe	Xxx	NHMe		
L-Ala-NHMe ( <b>19</b> )	<i>trans</i>	7.33 (7.32)	6.97 (7.05)	0.30 –	0.05 –	5 (–) <sup>[d]</sup>	1.76 (–) <sup>[d]</sup>
	<i>cis</i>	7.60 (–) <sup>[d]</sup>	6.65 (–) <sup>[d]</sup>	–	–	–	–
L-Val-NHMe ( <b>20</b> )	<i>trans</i>	7.20 (7.61)	6.29 (7.83)	0.11 –	1.12 –	54 (11)	–0.09 (1.25)
	<i>cis</i>	7.50 (8.15)	7.23 (7.47)	0.20 –	0.19 –	–	–
L-Leu-NHMe ( <b>21</b> )	<i>trans</i>	7.21 (7.72)	6.61 (7.67)	0.22 –	0.69 –	53 (19)	–0.07 (0.87)
	<i>cis</i>	7.61 (8.41)	7.01 (7.53)	0.34 –	0.21 –	–	–
L-Phe-NHMe ( <b>22</b> )	<i>trans</i>	6.55 (7.76)	6.58 (7.69)	0.64 –	0.74 –	62 (31)	–0.29 (0.48)
	<i>cis</i>	7.57 (8.53)	7.20 (7.58)	0.49 –	0.20 –	–	–
Aib-NHMe ( <b>23</b> )	<i>trans</i>	6.45 (8.21)	7.25 (7.46)	1.41 –	0.30 –	32 (8)	0.45 (1.46)
	<i>cis</i>	7.20 (7.90)	7.15 (7.25)	0.26 –	0.10 –	–	–
L-Ala-OMe ( <b>16</b> )	<i>trans</i>	7.12 (8.20)	– (–)	0.59 –	–	56 (21)	–0.14 (0.79)
	<i>cis</i>	8.98 (8.82)	– (–)	–0.03 –	–	–	–
L-Val-OMe ( <b>17</b> )	<i>trans</i>	7.34 (8.01)	– (–)	0.30 –	–	21 (11)	0.79 (1.25)
	<i>cis</i>	8.92 (8.69)	– (–)	–0.04 –	–	–	–
L-Phe-OMe ( <b>18</b> )	<i>trans</i>	7.13 (8.13)	– (–)	0.37 –	–	67 (33)	–0.42 (0.42)
	<i>cis</i>	9.13 (9.00)	– (–)	–0.01 –	–	–	–

[a] The values in parentheses correspond to those in [D<sub>6</sub>]DMSO. [b] Δδ is chemical shift difference for NH protons in CDCl<sub>3</sub> and 21.7% [D<sub>6</sub>]DMSO/CDCl<sub>3</sub>. [c] Δ*G* [kcal mol<sup>–1</sup>] at 300 K. [d] Below the observable limit of the present measurement.

Indeed, in the case of L-Xxx = L-Val (**20**), L-Leu (**21**) and L-Phe (**22**), the *cis* conformer is populated to a greater extent than the *trans* form. Figure 9 provides a comparison of partial NOE spectra, C<sup>α</sup>H⇌C<sup>β</sup>H region which highlights the difference between L-Ala (**19**) and L-Phe (**22**) peptides. The crystal structure of Piv-L-Pro-L-Pro-L-Phe-OMe (**18**) revealed that both molecules in the asymmetric unit adopt type VIa conformations, with Pro(1)–Pro(2) having a *cis* geometry.

The solvent dependence data in Figure 8 (see also Δδ values in Table 4), revealed that in the *trans* form, two solvent shielded NH groups appear to be present only in the case of L-Xxx = L-Ala (**19**). In the case of L-Xxx = L-Val (**20**), L-Leu (**21**) and L-Phe (**22**), the methylamide NH of the *trans* form shows considerable solvent dependence, indicative of a significant fraction of non-hydrogen bonded conformations. There is a marked difference in the degree of exposure of L-Xxx NH and methylamide NH in case of L-Val (**20**) and L-Leu (**21**) peptides, whereas the two NH groups appear to be more solvent exposed in the case of L-Phe

(**22**). In the case of Xxx = Aib (**23**), it is the Aib NH which shows a larger solvent dependence (Δδ = 1.41 ppm), while the methylamide NH is hydrogen bonded (Δδ = 0.30 ppm). This is undoubtedly a consequence of the formation of a Pro(2)-Aib(3) β-turn conformation, which has been widely characterized in crystal structure of short peptides.<sup>[1b]</sup> In all cases, the extent of solvent dependence in the case of *cis* conformers is much less for both the sets of NH protons. A type VI β-turn conformation,<sup>[22f,h,27]</sup> which might be anticipated with L-Pro-L-Pro-L-Xxx sequences with Pro-Pro *cis* geometry, is expected to result in solvent shielding of the L-Xxx NH protons.

A notable feature of the data in Table 4 for the tripeptide N-methylamide in CDCl<sub>3</sub> is that the percentage of the *cis* form exceeds that of the *trans* conformer in case of L-Xxx = L-Val (**20**), L-Leu (**21**) and L-Phe (**22**). In contrast, for Xxx = Aib (**23**), there is considerable reduction in the population of *cis* form and most dramatically for L-Xxx = L-Ala (**19**), the *cis* population drops to ~5%. Thus, the nature of L-

Xxx residue has a profound effect on free energy differences between the Pro-Pro *cis* and *trans* form. Interestingly, in [D<sub>6</sub>]DMSO, there is a substantial reduction in the population of *cis* conformer in all the cases. Indeed, in case of L-Xxx = L-Ala, the *cis* form is undetectable. In earlier studies of model peptides the population of X-Pro *cis* conformer has been shown to increase in polar solvents.<sup>[28]</sup> Clearly, in the series Piv-L-Pro-L-Pro-L-Xxx-NHMe, the stabilization of the *cis* form in an apolar solvent like CDCl<sub>3</sub> is undoubtedly driven by the favourable energy of formation of an intramolecular 4→1 hydrogen bond in a type VI β-turn conformation. The effect of the alanine side chain is particularly noteworthy, in that an all *trans*, incipient 3<sub>10</sub> helix is stabilized. Interestingly, in the corresponding ester Piv-L-Pro-L-Pro-L-Ala-OMe, the *cis* conformer is populated to the extent of 56% in CDCl<sub>3</sub>, clearly suggesting that the formation of second hydrogen bond is critical in promoting an all *trans* structure in the corresponding N-methylamide (**19**).

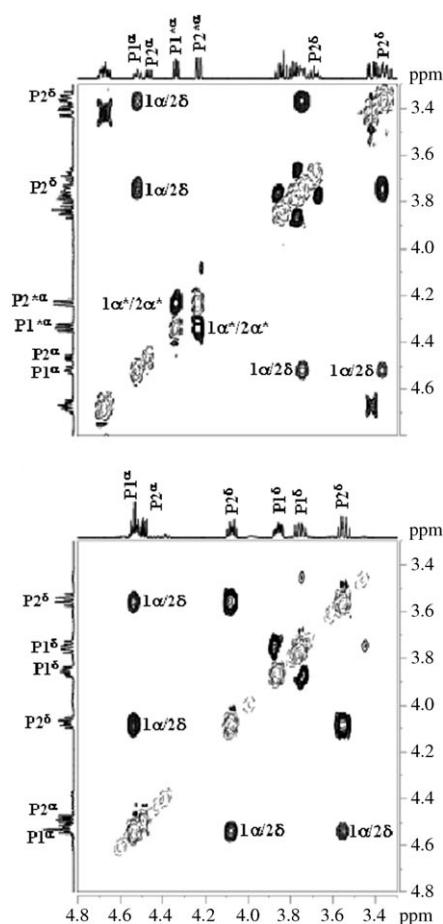


Figure 9. Partial 500 MHz NOESY spectra of the peptides Piv-L-Pro-L-Pro-L-Phe-NHMe (**22**) (top) and Piv-L-Pro-L-Pro-L-Ala-NHMe (**19**) (bottom) illustrating Pro(1) C $\alpha$ H $\leftrightarrow$  Pro(2) C $\alpha$ H and Pro(1) C $\alpha$ H $\leftrightarrow$  Pro(2) C $\beta$ H in CDCl<sub>3</sub>. \* Corresponds to *cis* conformation

## Conclusion

Polypeptide chain folding can be directed by the imposition of local backbone constraints.<sup>[4]</sup> Restricting short segments to a limited range of conformational excursions permits the nucleation of ordered structures. For example, type I/III  $\beta$ -turns can serve as a nucleus for helical folding, with the formation of an incipient  $3_{10}$  helix when two contiguous turns occur over a three residue segment, with the central residue being shared between the two turns. Prime  $\beta$ -turns like type I' and II' serve as nuclei for the generation of registered  $\beta$ -hairpin structures. Diproline segments can adopt only a limited range of conformations and are accommodated into specific  $\beta$ -turn structures. In segments where the residues alternate in chirality (heterochiral diproline segments), type II  $\beta$ -turns are strongly favored:  $\beta_{II'}$  in the case of D-L segments and  $\beta_{II}$  in the case of L-D units. In homochiral L-Pro-L-Pro sequences, the tendency to form type I/III turns competes with the formation of semi-extended polyproline structures. In both the homochiral and heterochiral diproline sequences, the nature of the flanking residue has a profound influence on the conformation of the diproline segment. In the

case of D-Pro-L-Pro sequences, a variety of L-residues placed at the C-terminus result in the formation of consecutive  $\beta$ -turn structures ( $\beta_{II-i}$ ) stabilized by the formation of two intramolecular 4 $\rightarrow$ 1 hydrogen bonds. In contrast, when the C-terminus residue has the D-configuration, the structures obtained are diverse. Notably, in the case of Piv-D-Pro-L-Pro-D-Ala-NHMe, a 5 $\rightarrow$ 1 hydrogen bonded  $\alpha$ -turn ( $C_{13}$ ) structure is obtained. Proline peptides are also well disposed towards adopting *cis* conformations about the Xaa-Pro peptide bond. In the present study, *cis* pro-pro bonds have been crystallographically characterized in two cases, one homochiral and the other heterochiral. In the case of Piv-L-Pro-L-Pro-L-Phe-OMe a type VIa  $\beta$ -turn conformation is observed whereas in Piv-D-Pro-L-Pro-D-Val-NHMe a structure devoid of any intramolecular hydrogen bond is observed with the D-Pro-L-Pro peptide bond being *cis*. The ability to probe the conformational space available to diproline segments is enhanced by the structural analysis of racemates in which packing effects are different from those anticipated in the case of crystals of pure enantiomers.

NMR studies in solution provide a means of characterizing multiple conformational states. In the present study, D-Pro-L-Pro-L-Xxx sequences have been shown to be largely conformationally homogeneous with the consecutive  $\beta$ -turn also being maintained in solution. In sharp contrast, in the L-Pro-L-Pro-L-Xxx series, the nature of the L-Xxx residue has a significant effect on the *cis-trans* equilibrium about the Pro-Pro peptide bond. L-Xxx = L-Ala is the only case where the population of the *cis* conformers is extremely small (5% in CDCl<sub>3</sub>). In all the other cases examined, *cis* forms predominate in an apolar medium CDCl<sub>3</sub>, presumably because of the formation of type VIa  $\beta$ -turn conformations which are stabilized by a single 4 $\rightarrow$ 1 intramolecular hydrogen bond. In polar solvents like DMSO that compete for hydrogen bonding backbone sites, the population of *cis* conformers shows a dramatic decrease. The results of the present study provide a detailed view of the possible conformational states of heterochiral and homochiral diproline sequences. The results also suggest that diproline segments can be effectively used in the design of short well-structured peptide sequences, especially when the role of the C-terminus flanking residue is appreciated. The successful design of a  $\beta$ -hairpin peptide with a three residue connecting loop is an illustrative example of this approach.<sup>[2c]</sup> The body of evidence presented in this paper on the conformations of model peptides containing diproline sequences suggests that unanticipated structures may yet be revealed by X-ray diffraction analysis of short peptides. The results also emphasize the subtle role of sequence effects in modulating the conformations of short, constrained peptide segments.

## Experimental Section

**Peptide synthesis:** All the peptides reported were synthesized by conventional solution phase methods using a fragment condensation strategy. The pivaloyl (Piv) group was used for the N-terminus, while the C-termini-

nus was protected as an N-methylamide. Couplings were mediated by dicyclohexylcarbodiimide/1-hydroxybenzotriazole (DCC/HOBT).<sup>[29]</sup> All the intermediates were characterized by <sup>1</sup>H NMR (80 MHz) and TLC (silica gel, chloroform/methanol 9:1) and were used without further purification. The final peptides were purified by silica-gel column chromatography followed by HPLC (C<sub>18</sub>, 5–10 $\mu$ m), employing methanol/water gradients. The homogeneity of the purified peptides was ascertained by analytical HPLC. The purified peptides were characterized by electrospray ionization mass spectrometry.<sup>[29]</sup>

**X-ray diffraction:** Single crystals suitable for X-ray diffraction were obtained by slow evaporation from petroleum ether/ethyl acetate and methanol/water mixtures. X-ray diffraction data were collected at room temperature on a Bruker AXS SMART APEX CCD diffractometer using MoK $\alpha$  radiation ( $\lambda=0.71073$  Å). All the structures were solved by direct methods using SHELXS-97<sup>[30a]</sup> and refined against  $F^2$ , with full-matrix least-squares methods using SHELXL-97.<sup>[30b]</sup> The crystal and diffraction parameters and refinement statistics for 14 peptide crystal structures are provided as Supporting Information (Table S2, Supporting Information). CCDC 645999 (1), 646000 (2), 646001 (3), 646002 (4), 646003 (5), 646004 (6), 646005 (7), 646006 (8), 646007 (10), 646008 (11), 646009 (15), 646010 (18), 646011 (20) and 646012 (23) contain the supplementary crystallographic data for this paper. These data can be obtained free of charge from The Cambridge Crystallographic Data Centre via www.ccdc.cam.ac.uk/data\_request/cif.

**NMR spectroscopy:** NMR experiments were carried out on a Bruker DRX500 spectrometer. 1D and 2D spectra were recorded at a peptide concentration of ~3 mM in CDCl<sub>3</sub>, at 300 K. Delineation of exposed NH groups was achieved by titrating a CDCl<sub>3</sub> solution with low concentrations of DMSO-*d*<sub>6</sub>. Resonance assignments were carried out with the help of 1D and 2D spectra. Residue specific assignments were obtained from TOCSY experiments, while NOESY/ROESY spectra permitted sequence specific assignments. All 2D experiments were recorded in phase sensitive mode using the TPPI (time proportional phase incrementation) method. A data set of 1024 $\times$ 450 was used for acquiring the data. The same data set was zero filled to yield a data matrix of size 2048 $\times$ 1024 before Fourier transformation. A spectral width of 6000 Hz was used in both dimensions. Mixing times of 100 and 200 ms were used for TOCSY and ROESY, respectively. Shifted square sine bell windows were used while processing. All processing was done using BRUKER XWINNMR software.

## Acknowledgement

Research in this area has been funded by a grant from the Council of Scientific and Industrial Research, India and a program grant from the Department of Biotechnology, India in the area of Molecular Diversity and Design. X-ray diffraction data were collected on the CCD facility funded under the IRHPA program of the Department of Science and Technology, India. S.A and R.R thank the Council of Scientific and Industrial Research, India, and the Department of Biotechnology, India for Research Associateships. B. C thanks Prof. R. Balaji Rao and Prof. R. L. Gupta (Banaras Hindu University, Varanasi, India) for their interest and encouragement.

- [1] a) Y. V. Venkatachalapathi, P. Balam, *Nature* **1979**, *281*, 83–84; b) R. Rai, S. Aravinda, K. Kanagarajadurai, S. Raghothama, N. Shamala, P. Balam, *J. Am. Chem. Soc.* **2006**, *128*, 7916–7928; c) D. S. Kemp, J. G. Boyd, C. C. Muendel, *Nature* **1991**, *352*, 451–454; d) D. S. Kemp, T. P. Curran, J. G. Boyd, T. J. Allen, *J. Org. Chem.* **1991**, *56*, 6683–6697; e) D. S. Kemp, T. P. Curran, W. M. Davis, J. G. Boyd, C. Muendel, *J. Org. Chem.* **1991**, *56*, 6672–6682.
- [2] a) J. A. Robinson, *Synlett* **2000**, 429–441; b) R. M. Hughes, M. L. Waters, *Curr. Opin. Struct. Biol.* **2006**, *16*, 514–524; c) R. Rai, S. Raghothama, P. Balam, *J. Am. Chem. Soc.* **2006**, *128*, 2675–2681; d) L. A. Haines, K. Rajagopal, B. Ozbas, D. A. Salick, D. J. Pochan,

- J. P. Schneider, *J. Am. Chem. Soc.* **2005**, *127*, 17025–17029; e) R. Fasan, R. L. A. Dias, K. Moehle, O. Zerbe, D. Obrecht, P. R. E. Mittl, M. G. Grutter, J. A. Robinson, *ChemBioChem* **2006**, *7*, 515–526; f) J. Spath, F. Stuart, L. Jiang, J. A. Robinson, *Helv. Chim. Acta* **1998**, *81*, 1726–1738; g) L. Jiang, K. Moehle, B. Dhanapal, D. Obrecht, J. A. Robinson, *Helv. Chim. Acta* **2000**, *83*, 3097–3112; h) M. Favre, K. Moehle, L. Jiang, B. Pfeiffer, J. A. Robinson, *J. Am. Chem. Soc.* **1999**, *121*, 2679–2685; i) A. Descours, K. Moehle, A. Renard, J. A. Robinson, *ChemBioChem* **2002**, *3*, 318–323; j) S. C. Shankaramma, K. Moehle, S. James, J. W. Vrijbloed, D. Obrecht, J. A. Robinson, *Chem. Commun.* **2003**, 1842–1843; k) Z. Athanasios, R. L. A. Dias, K. Moehle, N. Dobson, G. Varani, J. A. Robinson, *J. Am. Chem. Soc.* **2004**, *126*, 6906–6913; l) J. K. Kretsinger, L. A. Haines, B. Ozbas, D. J. Pochan, J. P. Schneider, *Biomaterials* **2005**, *26*, 5177–5186; m) B. Ozbas, K. Rajagopal, J. P. Schneider, D. J. Pochan, *Phys. Rev. Lett.* **2004**, *93*, 268106; n) L. A. Haines, K. Rajagopal, B. Ozbas, D. A. Salick, D. J. Pochan, J. P. Schneider, *J. Am. Chem. Soc.* **2005**, *127*, 17025–17029; o) S. Hanessian, M. Angiolini, *Chem. Eur. J.* **2002**, *8*, 111–117.
- [3] a) P. Y. Chou, G. D. Fasman, *J. Mol. Biol.* **1977**, *115*, 135–175; b) C. M. Wilmot, J. M. Thornton, *J. Mol. Biol.* **1988**, *203*, 221–232; c) G. D. Rose, L. M. Gierasch, J. A. Smith, *Adv. Protein Chem.* **1985**, *37*, 1–109; d) J. S. Richardson, D. C. Richardson, In *Prediction of Protein Structure and the Principles of Protein Conformation* (Ed.: G. D. Fasman), Plenum Press, New York, **1989**, pp. 1–98.
- [4] a) W. F. DeGrado, *Adv. Protein Chem.* **1988**, *39*, 51–124; b) J. S. Richardson, *Adv. Protein Chem.* **1981**, *34*, 167–339; c) J. Venkatraman, S. C. Shankaramma, P. Balam, *Chem. Rev.* **2001**, *101*, 3131–3152; d) S. Aravinda, N. Shamala, R. S. Roy, P. Balam, *Proc. Indian Acad. Sci. (Chem. Sci.)* **2003**, *115*, 373–400.
- [5] a) P. R. Schimmel, P. J. Flory, *J. Mol. Biol.* **1968**, *34*, 105–120; b) B. Robson, E. Suzuki, *J. Mol. Biol.* **1976**, *107*, 327–356; c) P. Y. Chou, G. D. Fasman, *Biochemistry* **1974**, *13*, 211–222; d) P. Y. Chou, G. D. Fasman, *Adv. Enzymol. Relat. Areas Mol. Biol.* **1978**, *47*, 45–148; e) M. Levitt, *Biochemistry* **1978**, *17*, 4277–4285; f) C. K. Smith, J. M. Withka, L. Regan, *Biochemistry* **1994**, *33*, 5510–5517.
- [6] a) L. G. Presta, G. D. Rose, *Science* **1988**, *240*, 1632–1641; b) J. S. Richardson, D. C. Richardson, *Science* **1988**, *240*, 1648–1652; c) R. Aurora, G. D. Rose, *Protein Sci.* **1998**, *7*, 21–38; d) K. Gunasekaran, H. A. Nagarajaram, C. Ramakrishnan, P. Balam, *J. Mol. Biol.* **1998**, *275*, 917–932; e) A. R. Viguera, L. Serrano, *Protein Sci.* **1999**, *8*, 1733–1742.
- [7] a) C. Soto, E. M. Sigurdsson, L. Morelli, R. A. Kumar, E. M. Castano, B. Frangione, *Nat. Med.* **1998**, *4*, 822–826; b) L. D. Estrada, C. Soto, *Curr. Top. Med. Chem.* **2007**, *7*, 115–126.
- [8] a) C. M. Venkatachalam, *Biopolymers* **1968**, *6*, 1425–1436; b) For a subsequent extension to the stereochemical analysis of homo and heterochiral two residue turns see: R. Chandrasekaran, A. V. Lakshminarayan, U. V. Pandya, G. N. Ramachandran, *Biochim. Biophys. Acta Protein Struct.* **1973**, *303*, 14–27.
- [9] a) G. E. Job, B. Heitmann, R. J. Kennedy, S. M. Walker, D. S. Kemp, *Angew. Chem.* **2004**, *116*, 5767–5769; *Angew. Chem. Int. Ed.* **2004**, *43*, 5649–5651; b) B. Heitmann, G. E. Job, R. J. Kennedy, S. M. Walker, D. S. Kemp, *J. Am. Chem. Soc.* **2005**, *127*, 1690–1704.
- [10] a) S. Hanessian, G. Papeo, M. Angiolini, K. Fettes, M. Beretta, A. Munro, *J. Org. Chem.* **2003**, *68*, 7204–7218; b) S. Hanessian, H. Sailes, A. Munro, E. Therrien, *J. Org. Chem.* **2003**, *68*, 7219–7233; c) S. Hanessian, G. Papeo, K. Fettes, E. Therrien, M. T. P. Viet, *J. Org. Chem.* **2004**, *69*, 4891–4899.
- [11] a) S. K. Awasthi, S. Raghothama, P. Balam, *Biochem. Biophys. Res. Commun.* **1995**, *216*, 375–381; b) I. L. Karle, S. K. Awasthi, P. Balam, *Proc. Natl. Acad. Sci. USA* **1996**, *93*, 8189–8193; c) S. R. Raghothama, S. K. Awasthi, P. Balam, *J. Chem. Soc. Perkin Trans. 2* **1998**, 137–143; d) T. S. Haque, J. C. Little, S. H. Gellman, *J. Am. Chem. Soc.* **1996**, *118*, 6975–6985; e) T. S. Haque, S. H. Gellman, *J. Am. Chem. Soc.* **1997**, *119*, 2303–2304; f) J. F. Espinosa, S. H. Gellman, *Angew. Chem.* **2000**, *112*, 2420–2423; *Angew. Chem. Int. Ed.* **2000**, *39*, 2330–2333; g) H. E. Stanger, S. H. Gellman, *J. Am. Chem. Soc.* **1998**, *120*, 4236–4237; h) S. H. Gellman, *Curr. Opin. Chem.*

- Biol.* **1998**, *2*, 717–725; i) D. Ramadan, D. J. Cline, S. Bai, C. Thorpe, J. P. Schneider, *J. Am. Chem. Soc.* **2007**, *129*, 2981–2988.
- [12] a) I. L. Karle, H. N. Gopi, P. Balaram, *Proc. Natl. Acad. Sci. USA* **2002**, *99*, 5160–5164; b) S. Aravinda, V. V. Harini, N. Shamala, C. Das, P. Balaram, *Biochemistry* **2004**, *43*, 1832–1846; c) V. V. Harini, S. Aravinda, R. Rai, N. Shamala, P. Balaram, *Chem. Eur. J.* **2005**, *11*, 3609–3620.
- [13] a) C. Das, S. Raghothama, P. Balaram, *J. Am. Chem. Soc.* **1998**, *120*, 5812–5813; b) C. Das, S. Raghothama, P. Balaram, *Chem. Commun.* **1999**, 967–968; c) J. Venkatraman, G. A. Nagana Gowda, P. Balar- am, *J. Am. Chem. Soc.* **2002**, *124*, 4987–4994; d) H. L. Schenck, S. H. Gellman, *J. Am. Chem. Soc.* **1998**, *120*, 4869–4870; e) J. D. Fisk, S. H. Gellman, *J. Am. Chem. Soc.* **2001**, *123*, 343–344; f) J. D. Fisk, M. A. Schmitt, S. H. Gellman, *J. Am. Chem. Soc.* **2006**, *128*, 7148–7149; g) C. M. Santiveri, J. Santoro, M. Rico, M. A. Jimenez, *Protein Sci.* **2004**, *13*, 1134–1147; h) C. Das, V. Nayak, S. Raghotha- ma, P. Balaram, *J. Pept. Res.* **2000**, *56*, 307–317.
- [14] C. M. Nair, M. Vijayan, Y. V. Venkatachalapathi, P. Balaram, *J. Chem. Soc. Chem. Commun.* **1979**, 1183–1184.
- [15] G. Zanotti, A. Bassetto, R. Battistutta, C. Folli, P. Arcidiaco, M. Stoppini, R. Berni, *Biochim. Biophys. Acta Protein Struct. Mol. En- zymol.* **2000**, *1478*, 232–238.
- [16] a) Y. Takeuchi, G. R. Marshall, *J. Am. Chem. Soc.* **1998**, *120*, 5363– 5372; b) D. K. Chalmers, G. R. Marshall, *J. Am. Chem. Soc.* **1995**, *117*, 5927–5937.
- [17] A preliminary report describing the crystal structure determination of peptide racemates (**12**, **13** and **14**) has been presented [I. Saha, B. Chatterjee, N. Shamala, P. Balaram, *Biopolymers (Peptide Sci.)* in press].
- [18] H. Nishihara, K. Nishihara, T. Uefuji, N. Sakota, *Bull. Chem. Soc. Jpn.* **1975**, *48*, 553–555.
- [19] a) D. V. Nataraj, N. Srinivasan, R. Sowdhamini, C. Ramakrishnan, *Curr. Sci.* **1995**, *69*, 434–447; b) V. Pavone, G. Gaeta, A. Lombardi, F. Natri, O. Maglio, C. Isernia, M. Saviano, *Biopolymers* **1996**, *38*, 705–721; c) B. Dasgupta, L. Pal, G. Basu, P. Chakrabarti, *Proteins* **2004**, *55*, 305–315.
- [20] P. N. Lewis, F. A. Momany, H. A. Scheraga, *Biochim. Biophys. Acta Protein Struct.* **1973**, *303*, 211–229.
- [21] H.-B. Kraatz, D. M. Leek, A. Houmam, G. D. Enright, J. Luszyk, D. D. M. Wayner, *J. Organomet. Chem.* **1999**, *589*, 38–49.
- [22] a) C. Grathwohl, K. Wüthrich, *Biopolymers* **1976**, *15*, 2025–2041; b) C. Grathwohl, K. Wüthrich, *Biopolymers* **1981**, *20*, 2623–2633; c) D. E. Stewart, A. Sarkar, J. E. Wampler, *J. Mol. Biol.* **1990**, *214*, 253–260; d) M. W. MacArthur, J. M. Thornton, *J. Mol. Biol.* **1991**, *218*, 397–412; e) D. Pal, P. Chakrabarti, *J. Mol. Biol.* **1999**, *294*, 271– 288; f) W.-J. Wu, D. P. Raleigh, *Biopolymers* **1998**, *45*, 381–394; g) C. M. Taylor, R. Hardre, P. J. B. Edwards, J. H. Park, *Org. Lett.* **2003**, *5*, 4413–4416; h) H. Y. Meng, K. M. Thomas, A. E. Lee, N. J. Zondlo, *Biopolymers (Peptide Sci.)* **2006**, *84*, 192–204.
- [23] a) G. N. Ramachandran, A. V. Lakshminarayanan, R. Balasubrama- nian, G. Tegoni, *Biochim. Biophys. Acta Protein Struct.* **1970**, *221*, 165–181; b) T. Ashida, M. Kakudo, *Bull. Chem. Soc. Jpn.* **1974**, *47*, 1129–1133; c) S. Tanaka, H. A. Scheraga, *Macromolecules* **1974**, *7*, 698–705; d) F. A. Momany, R. F. McGuire, A. W. Burgess, H. A. Scheraga, *J. Phys. Chem.* **1975**, *79*, 2361–2381; e) D. Cremer, J. A. Pople, *J. Am. Chem. Soc.* **1975**, *97*, 1354–1358; f) D. F. De Tar, N. P. Luthra, *J. Am. Chem. Soc.* **1977**, *99*, 1232–1244; g) V. Madison, *Bio- polymers* **1977**, *16*, 2671–2692; h) B. K. Ho, E. A. Coutsiias, C. Seok, K. A. Dill, *Protein Sci.* **2005**, *14*, 1011–1018; i) E. J. Milner-White, L. H. Bell, P. H. Maccallum, *J. Mol. Biol.* **1992**, *228*, 725–734; j) L. Vitagliano, R. Berisio, A. Mastrangelo, L. Mazzarella, A. Zagari, *Protein Sci.* **2001**, *10*, 2627–2632.
- [24] F. H. Allen, *Acta Crystallogr. Sect. B* **2002**, *58*, 380–388.
- [25] S. Donnini, G. Groenhof, R. K. Wierenga, A. H. Juffer, *Proteins* **2006**, *64*, 700–710.
- [26] a) I. Z. Siemion, T. Wieland, K.-H. Pook, *Angew. Chem.* **1975**, *87*, 712–714; *Angew. Chem. Int. Ed. Engl.* **1975**, *14*, 702–703; b) D. E. Dorman, F. A. Bovey, *J. Org. Chem.* **1978**, *38*, 2379–2383; c) R. Ri- charz, K. Wüthrich, *Biopolymers* **1978**, *17*, 2133–2141.
- [27] a) J. Yao, R. Bruschweiler, H. J. Dyson, P. E. Wright, *J. Am. Chem. Soc.* **1994**, *116*, 12051–12052; b) J. Yao, H. J. Dyson, P. E. Wright, *J. Mol. Biol.* **1994**, *243*, 754–766; c) J. Yao, V. A. Feher, B. F. Espejo, M. T. Reymond, P. E. Wright, H. J. Dyson, *J. Mol. Biol.* **1994**, *243*, 736–753; d) L. Halab, W. D. Lubell, *J. Am. Chem. Soc.* **2002**, *124*, 2474–2484.
- [28] a) V. Madison, J. Schellman, *Biopolymers* **1970**, *9*, 511–567; b) T. Hi- gashijima, M. Tasumi, T. Miyazawa, *Biopolymers* **1977**, *16*, 1259– 1270.
- [29] Synthetic procedures and ESI-MS spectra are provided as Support- ing Information.
- [30] a) G. M. Sheldrick, *SHELXS-97*, A program for automatic solution of crystal structures, University of Göttingen, Göttingen (Germany), **1997**; b) G. M. Sheldrick, *SHELXL-97*, A program for the refine- ment of crystal structures, University of Göttingen, Göttingen (Ger- many), **1997**.

Received: December 22, 2007  
Published online: May 19, 2008